HHS Public Access

Author manuscript

Clin Nucl Med. Author manuscript; available in PMC 2019 September 01.

Published in final edited form as:

Clin Nucl Med. 2018 September ; 43(9): 663–669. doi:10.1097/RLU.0000000000002209.

^{68}Ga-NOTA-RM26 PET/CT in the Evaluation of Breast Cancer: A Pilot Prospective Study

Jie Zang, MD[1,2], **Feng Mao, MD**[3,*], **Hao Wang, MD**[1,2], **Jingjing Zhang, MD**[1,2], **Qingxing Liu, MD**[1,2], **Li Peng, MD**[3], **Fang Li, MD**[1,2], **Lixin Lang, PhD**[4], **Xiaoyuan Chen, PhD**[4,*], and **Zhaohui Zhu, MD, PhD**[1,2,*]

[1]Department of Nuclear Medicine, Peking Union Medical College (PUMC) Hospital, Chinese Academy of Medical Science and PUMC, Beijing 100730, China

[2]Beijing Key Laboratory of Molecular Targeted Diagnosis and Therapy in Nuclear Medicine, Beijing 100730, China

[3]Department of Breast Surgery, Peking Union Medical College (PUMC) Hospital, Chinese Academy of Medical Science and PUMC, Beijing 100730, China

[4]Laboratory of Molecular Imaging and Nanomedicine (LOMIN), National Institute of Biomedical Imaging and Bioengineering (NIBIB), National Institutes of Health (NIH), Bethesda, Maryland, 20892, USA

Abstract

This prospective pilot study investigated the value of ^{68}Ga-NOTA-RM26, an antagonist targeting gastrin-releasing peptide receptor (GRPR), in evaluation of breast cancer.

Methods—Thirty-five women in suspicion of breast cancer based on mammography or ultrasonography were recruited with informed consent. They underwent PET/CT scans 30 min after intravenous injection of ^{68}Ga-NOTA-RM26 in a dose of 1.85 MBq (0.05 mCi) per kilogram body weight within 1 week before surgery. The ^{68}Ga-NOTA-RM26 uptake was correlated with the pathological and immunohistochemical findings.

Results—^{68}Ga-NOTA-RM26 positivity was found correlated with estrogen receptor (ER) expression ($P = 0.006$) and menstrual status ($P = 0.019$). In 34 patients diagnosed with breast cancer, the SUV_{max} was found significantly higher in the ER-positive breast cancer (4.97 ± 1.89) than in the ER-negative breast cancer (2.78 ± 0.65, $P < 0.001$). ^{68}Ga-NOTA-RM26 was also found accumulated in normal breast tissue, with the SUV_{max} significantly higher in patients at the secretory phase of menstrual cycle (2.27 ± 0.71) than in those at the non-secretory phase (1.59 ± 0.49, $P = 0.017$) and post-menopause (1.43 ± 0.44, $P = 0.002$). If the secretory phase patients were excluded, the sensitivity, specificity, and accuracy for differentiation of breast cancer from breast tissue increased from 85.3%, 86.8%, and 86.1% to 100.0%, 90.9%, and 95.5%, respectively.

Conclusion—This pilot study indicated that the diagnostic accuracy of ^{68}Ga-NOTA-RM26 PET/CT in breast cancer may correlate with ER expression and menstrual status of the patient. It

*Corresponding authors: Feng Mao (mmc8941@me.com); Zhaohui Zhu (13611093752@163.com); Xiaoyuan Chen (Shawn.Chen@nih.gov).

may be better to avoid performing this examination during the menstrual secretory phase to reduce physiological uptake in normal breast tissue.

Keywords

^{68}Ga-NOTA-RM26; breast cancer; gastrin-releasing peptide receptor antagonist; PET/CT

Introduction

Breast cancer is a leading cause of cancer-related death found in women worldwide, with a steadily increasing incidence in many countries over the past 30 years [1-4]. Thus, early detection and thorough evaluation of primary breast cancer and its metastases may lead to a higher rate of successful treatment and extend the patient's life span.

Currently, the diagnosis of breast cancer is usually determined by anatomical imaging, such as X-ray mammography (XMM), ultrasound (US), magnetic resonance imaging (MRI), and is confirmed *via* biopsy. With the advent of molecular imaging, nuclear medicine techniques are considered to hold promise for the early detection of tumors through a functional perspective, providing information on molecular characteristics.

The gastrin-releasing peptide receptor (GRPR) is known as a G-protein-coupled receptor that is expressed in a series of cancer types, including breast cancer, small cell lung cancer, prostate cancer, glioma and neuroblastoma [5-8]. According to literature, 62–96% of primary breast cancers express GRPR. GRPR is heterogeneously expressed in neoplastic epithelial mammary cells, ductal carcinomas in situ, and invasive carcinoma. GRPR is also expressed in metastatic lymph nodes from breast cancer, whereas the level of GRPR expression in normal lymph node tissue is very low [6, 9]. GRPR exhibited a predominantly intracytoplasmic expression in breast tumor cells and with concomitant immunoreactivity of the cell membrane. Recent studies have shown a preference for GRPR antagonists over GRPR agonists [10, 11]. Compared with receptor agonists, antagonists often show higher binding and more favorable pharmacokinetics [12].

The GRPR antagonist RM26 (D-Phe-Gln-Trp-Ala-Val-Gly-His-Sta-Leu-NH_2) was synthesized and conjugated to NOTA chelator *via* a short PEG spacer and labeled with ^{68}Ga. Tumor targeting and biodistribution studies of ^{68}Ga-NOTA-RM26 in mice bearing PC-3 human prostate cancer xenografts showed high and specific uptake in tumors and a high tumor-to-background ratio [13]. More recently, we proved that ^{68}Ga-NOTA-RM26 PET/CT was safe and useful in patients with prostate cancer [14]. However, its utility in the assessment of breast cancer has not been systemically explored. Thus, here we evaluated the diagnostic value of PET/CT using ^{68}Ga-NOTA-RM26 for patients with suspicious breast lesions as a pilot study, in order to verify its usefulness.

MATERIALS AND METHODS

Patients

This study was registered at clinicaltrials.gov (NCT03347864). With institutional review board approval and written informed consent, 35 women suspected of having 36 primary

breast cancers based on mammography or ultrasonography and not experienced any local or systemic therapies were recruited from November 2016 to April 2018 in Peking Union Medical College Hospital. The average patient age (mean ± standard deviation) was 49 ± 11 years (range 30–71 years). Among the patients, 23 were premenopausal women with regular menstrual cycles and the remaining 12 patients were post-menopausal women. The menstrual status was recorded on the day of performing ^{68}Ga-NOTA-RM26 PET/CT in premenopausal women. The patients' basic characteristics are listed in Table 1.

^{68}Ga-NOTA-RM26 PET/CT

Preparation of NOTA-RM26 and ^{68}Ga labeling were performed as described previously [13]. All patients underwent ^{68}Ga-NOTA-RM26 PET/CT acquisitions from upper thigh to chin using a Biograph 64 Truepoint TrueV TrueX system (Siemens Medical Solutions, Erlangen, Germany) at 30 min after intravenous injection of 1.85 MBq (0.05 mCi) per kilogram body weight of ^{68}Ga-NOTA-RM26 within 1 week before the surgery. The images from upper thigh to chin were acquired using a low-dose CT scan (120 kV, 35 mA, 512 × 512 matrix, 3-mm layer, 70 cm field of view). The PET scan of each patient covered in 5–6 bed positions (2 min/bed), with the arms held above the head and from the upper thigh to chin.

Immunohistochemistry

We examined the immunohistochemical features of the obtainable specimens in 20/35 cases. ER , PR and HER-2 status was determined according to published recommendations [15,16]. The representative samples of excised tumors and lymph nodes were fixed with 10% neutral buffered formalin and embedded in paraffin. Four-μm-thick tissue slices were incubated with rabbit anti-human polyclonal antibody against human GRPR (ab39963) after blocking and washing. Immunohistochemistry results for GRPR were independently evaluated by two experienced examiners and expressed as an immunoreactive score (IRS) in consideration of staining intensity and the percentage of positive tumor cells in the following way: 0, no staining; 1, weak staining; 2, moderate staining; and 3, strong staining. 0, no positive cells; 1, ≤ 10% positive cells; 2, 11–50% positive cells; 3, 51–80% positive cells; and 4, > 80% positive cells. Therefore, the final IRS score (staining intensity × percentage of positive cells) was in the range of 0 to 12. For the purpose of our study, no GRPR expression means IRS 0-1, weak GRPR expression means IRS 2-3, moderate GRPR expression refers to IRS 4-8 and strong GRPR expression refers to IRS 9-12.

PET/CT Image and Data Analysis

The PET/CT images were manipulated on a Siemens MMWP workstation. PET images were jointly analyzed by two experienced nuclear medicine physicians. For ^{68}Ga-NOTA-RM26 PET/CT imaging, PET positivity was defined as focal tracer uptake of the primary tumor or lymph nodes over the local background, in correlation with CT. The tumors with uptakes similar to or lower than breast tissue were defined as PET negative. The maximum and mean standardized uptake values (SUV_{max} and SUV_{mean}, respectively) in the volumes of interest were acquired through the software. The tumor-to-background (T/B) ratios were calculated for further analysis. The peripheral breast tissue was considered as background for calculation.

Statistical Analysis

Calculations were performed using SPSS software (IBM SPSS Statistics for Windows, Version 21.0; Armonk, NY). All quantitative data were expressed as mean ± standard deviation. A *P* value of less than 0.05 was accepted as statistically significant. SUV values were correlated with estrogen receptor (ER), human epidermal growth factor receptor 2 (Her-2), progesterone receptor (PR) status and the Ki-67 index in univariate analysis (Spearman's rho (ρ) for ordinal/continuous and *t*-test for nominal data). One-way ANOVA analysis was used to analyze the correlation of ^{68}Ga-NOTA-RM26 uptake in breast tissue with the menstrual cycle. The correlation between PET-positivity with ER status and the menstrual cycle was evaluated by Chi square test. ROC curve analysis was performed to determine an optimal cutoff for detecting breast cancer and breast tissue and to compare the diagnostic performance when the ER-negative patients or those in the secretory phase were removed. Furthermore, correlation analysis used the Spearman rank correlation test between the SUV values and the immunoreactive scores.

RESULTS

In the 35 patients, a total of 36 tumors were verified by surgery and pathology, including 27 invasive ductal cancer, 1 invasive lobular carcinoma, 4 intraductal carcinoma, 1 lobular carcinoma *in situ*, 1 mucinous carcinoma, and 2 fibroadenoma. Among the 34 lesions with breast cancer, 28 tumors were ER-positive, 27 tumors were PR-positive, 29 tumors in different level of Her-2 positivity. Eighteen patients were pathologically reported with ipsilateral lymph node metastasis and three patients only reported with micro-metastasis. No remarkable adverse event (dizziness, vomiting, abdominal discomfort) correlated with the study was reported in any of the enrolled patients within 2h after the administration.

^{68}Ga-NOTA-RM26 PET/CT in Detection of Primary Breast Cancer

Among the 34 patients with breast cancer, 29 primary tumors were clearly detected with elevated ^{68}Ga-NOTA-RM26 uptake as compared with the normal breast tissue and were rated as PET-positive (Fig. 1, Fig.2, and Fig 3). The SUV_{max} of PET-positive tumors was from 2.07 to 9.01 (4.88 ± 1.92), and the T/B ratios were from 1.62 to 17.09 (3.27 ± 2.82). Three tumors that could not be differentiated from breast tissue and two tumors that showed ^{68}Ga-NOTA-RM26 accumulation lower than the breast tissue were diagnosed as PET-negative (Fig. 4). The SUV_{max} of ^{68}Ga-NOTA-RM26 activity in PET-negative tumors was from 2.10 to 3.64 (2.94 ± 0.56), and the T/B ratios of ^{68}Ga-NOTA-RM26 accumulation were from 0.71 to 1.38 (1.08 ± 0.29). The SUV_{max} of ^{68}Ga-NOTA-RM26 activity in all 34 breast cancers was 4.58 ± 1.93. The two fibroadenomas could not be distinguished from the surrounding breast tissue and were thus defined as PET-negative. The SUV_{max} of the corresponding regions were 3.48 and 1.94, respectively.

PET positivity was associated with ER status ($P = 0.006$). 26/28 tumors with positive ER expression were diagnosed with PET-positive, in contast to 3/6 tumors with ER-negative expression rated PET-positive. The SUV_{max} in ER-positive tumors was 4.97 ± 1.89 as compared to 2.78 ± 0.65 in ER-negative tumors ($P < 0.001$) (Fig. 5A). However, no

correlations were found between SUV_{max} and the other relative biomarker expressions (i.e., PR, Her-2 status, and Ki-67 in percent).

The breast tissue showed intra- and inter-individual variability, moderately strong ^{68}Ga-NOTA-RM26 binding, with a SUV_{max} from 0.55 to 3.22 (1.80 ± 0.68) and a SUV_{mean} from 0.35 to 2.66 (1.18 ± 0.56. The intensity of ^{68}Ga-NOTA-RM26 uptake in the breast tissue was significantly associated with the menstrual cycle ($P = 0.002$ for SUV_{max}, and $P = 0.001$ for SUV_{mean}). Physiologic RM26 uptake in the breast tissue in patients at secretory phase (SUV_{max} 2.27 ± 0.71, n = 14) were significantly higher than those at the non-secretory phase (SUV_{max} 1.59 ± 0.49, n = 10; $P = 0.017$) and post-menopause (SUV_{max} 1.43 ± 0.44, n = 12; $P = 0.002$). Moreover, PET positivity was also associated with menstrual cycle ($P = 0.019$). 4/5 tumors rated PET-negative were examined during the secretory phase. In addition, the uterus showed ^{68}Ga-NOTA-RM26 uptake with moderate to intense densities in all phases of the menstrual cycle and post-menopause, with a SUV_{max} from 2.88 to 9.23 (5.01 ± 1.80) and a SUV_{mean} from 1.71 to 7.94 (3.18 ± 1.42).

ROC curve analysis showed the area under the curve for ^{68}Ga-NOTA-RM26 uptake level was 0.952 in breast tumor and breast tissue for the breast cancer patients. Optimal diagnostic cutoff value according to ROC analysis was 2.76. When a SUV_{max} of 2.76 was used as a cutoff, the resulting sensitivity, specificity, and accuracy were 85.3%, 86.8%, and 86.1%, respectively.

If the patients with ER-negative tumors were excluded, the area under the curve for ^{68}Ga-NOTA-RM26 uptake level was 0.977. Optimal diagnostic cutoff value according to ROC analysis was 3.29. When an optimal SUV_{max} of 3.29 was used as a cutoff, the resulting sensitivity, specificity, and accuracy for detection of ER-positive tumor were 85.7%, 96.9%, and 91.3%, respectively.

If the patients in the secretory phase of menstrual cycle were excluded, the area under the curve for ^{68}Ga-NOTA-RM26 uptake level reached 0.991. Optimal diagnostic cutoff value according to ROC analysis was 2.06. When an optimal SUV_{max} of 2.16 was used as a cutoff, the resulting sensitivity, specificity, and accuracy reached to 100.0%, 90.9%, and 95.5%, respectively.

Detection of Lymph Node Metastases

All patients underwent surgery and pathological examination confirmed that 18 patients had metastatic lymph nodes. ^{68}Ga-RM-26 PET/CT detected 46 metastatic lymph nodes in 15 patients (Fig. 1 and Fig.3), and the other 3 patients reported with micro-metastases in the lymph nodes were diagnosed as negative. The SUV_{max} of ^{68}Ga-NOTA-RM26 activity in metastatic lymph nodes was 2.61 ± 3.65, which was significantly higher than that in non-metastatic lymph nodes (0.65 ± 0.11, $P = 0.036$).

Immunohistochemistry of GRPR Expression

Forty representative samples of excised tumors and lymph nodes obtained from 20 patients, including 19 patients with breast cancer and 1 patient with breast fibrous tumor, were analyzed with immunohistochemical stain of GRPR expression. GRPR expression of breast

tumor was absent in 1 cases (5%), weak in 2 cases (10%), moderate in 14 cases (70%) and strong in 4 cases (20%). There was a significant positive correlation between SUV_{max} from ^{68}Ga-NOTA-RM26 PET/CT and GRPR expression with an immunoreactive score ($r = 0.805$, $P < 0.001$) (Fig. 5B).

DISCUSSION

Previous studies have confirmed that receptor imaging methods have great diagnostic usefulness and accuracy for breast tumors, although these are not used as often as the traditional methods [17, 18]. Breast cancer is a kind of tumor with high GRPR expression. Many studies have confirmed that GRPR antagonists or agonists are helpful for the detection and diagnosis of breast cancer, due to their high diagnostic performance. In this preliminary study, we investigated the efficacy of a GRPR antagonist, ^{68}Ga-NOTA-RM26, in patients with breast tumors. ^{68}Ga-NOTA-RM26 PET/CT was effective in visualizing GRPR expression with high contrast in a majority of the examined breast cancer patients (85%; 29/34). Additionally, the SUV_{max} of ^{68}Ga-NOTA-RM26 in ER-positive tumors was significantly higher than that in ER-negative tumors. There was a significant positive correlation between the SUV of ^{68}Ga-NOTA-RM26 and the expression levels of GRPR. Therefore, we hypothesized that ^{68}Ga-NOTA-RM26 imaging with high image quality is important for evaluating the expression of GRPR and may hold promise in breast cancer patients, especially for ER-positive tumors.

A series of studies of radiolabeled GRPR antagonists have been quite encouraging. In one study, ^{68}Ga-SB3 visualized lesions in four of six patients with advanced and metastatic breast cancer [19]. In another research, ^{68}Ga-RM2 showed that 13 of 18 primary breast tumors and several metastatic lesions were clearly visualized [20]. In the current work, ^{68}Ga-NOTA-RM26 PET/CT detected 29/34 tumors, and 15/18 cases of lymph node metastasis. These results suggest the potential value of GRPR PET imaging for the detection and diagnosis of breast cancer and lymph node metastasis.

In this study, the positive correlation between SUV_{max} obtained from ^{68}Ga-NOTA-RM26 and the ER status is consistent with the findings of a previous study that showed highly significant positive correlation between the binding capacities of high-affinity [Tyr^4]bombesin-binding sites and estrogen receptor level [21]. In addition, a retrospective study showed that GRPR overexpression was found in 75.8% tumors and was most strongly associated with ER positivity [22]. In our study, PET positivity was associated with ER status ($P = 0.006$). When excluding the cases with ER-negative tumors, the sensitivity, specificity, and accuracy for differentiation of breast cancer from normal breast tissue increased from 85.3%, 86.8%, and 86.1% to 85.7%, 96.9%, and 91.3%, respectively. It implies that ^{68}Ga-NOTA-RM26-PET/CT may be a promising imaging method in evaluation of breast cancer, especially for the ER-positive tumors.

Recent results of the GRPR antagonist ^{68}Ga-RM2 PET/CT imaging showed low to moderate uptake in normal breast tissue. Another study observed significant correlation between the intensity of FDG uptake in breast tissue and the menstrual cycle [23]. In this study, histopathology confirmed high expression of GRPR not only in tumor cells but also in breast

tissue, corroborating with ^{68}Ga-RM-26 PET/CT imaging. There was a significant correlation between the SUV value of ^{68}Ga-NOTA-RM26 in breast tissue and the menstrual cycle. Normal physiologic RM26 uptake in the secretory phase was higher than that in the non-secretory phase and in post-menopause, that may be caused by periodic changes in estrogen with proliferative actions and progestin with anti-estrogenic and secretory transforming actions [24, 25]. Our data suggest that women may have lower specificity for the detection of breast tumors on ^{68}Ga-NOTA-RM26 PET in the secretory phase than those in post-menopause and the non-secretory phase in premenopausal women and when excluding the cases in the secretory phase, there was an increased sensitivity, specificity, and accuracy from 85.3%, 86.8%, and 86.1% to 100.0%, 90.9%, and 95.5%, respectively. This means that the best time to perform ^{68}Ga-NOTA-RM26 PET/CT imaging may be the proliferative phase in premenopausal women. In addition, the uterus showed ^{68}Ga-NOTA-RM26 uptake with moderate to intense densities in all phases of the menstrual cycle and post menopause, corresponded with intense GRPR expression in uterus [26].

FDG PET/CT has high specificity but compromised sensitivity (24-82%) for identifying axillary nodal disease in breast cancer [27]. In this study, ^{68}Ga-NOTA-RM26 PET/CT detected lymph node metastasis in 15/18 (83.3%) patients, whereas the remaining 3 patients had only micro-metastasis in lymph nodes. The diameter of micro-metastatic foci was about 1 mm, which was difficult to be detected because of the 4–5 mm resolution of present clinical PET systems.

There were several limitations in our study. First, we studied a relatively low number of patients. The diagnostic parameters, such as sensitivity, specificity, and accuracy can be somewhat biased. Moreover, the cutoff value that differentiated best between breast tumor and breast tissue was not universally applicable to all patients. Second, breast tissue showed weak to moderately strong ^{68}Ga-NOTA-RM26 binding, especially in the secretory phase of the menstrual cycle, which could lead to difficulty in diagnosing breast cancer. Thirdly, there will be some errors as lymph nodes detected by ^{68}Ga-NOTA-RM26 PET/CT that do not completely correspond to the lymph nodes detected in immunohistochemistry, because we can only differentiate them by size and metastasis. However, based on the significant positive correlation between the SUV from ^{68}Ga-NOTA-RM26 PET/CT and GRPR expression of lymph nodes, the error might be small. Finally, to make a definite conclusion about the correlation between the SUV value of ^{68}Ga-NOTA-RM26 in breast tissue and the menstrual cycle, scans in different periods of menstrual cycle in the same patients may be needed.

Conclusions

This pilot study indicated that the diagnostic efficacy of ^{68}Ga-NOTA-RM26 PET/CT in breast cancer may correlate with the ER expression in the tumor and the menstrual status of the patient. To avoid intense physiological uptake of ^{68}Ga-NOTA-RM26 in normal breast tissue and increase the detection ability, it is recommended to avoid examination during the secretory phase of the menstrual cycle.

Acknowledgments

This work was supported by the Intramural Research Program of the National Institute of Biomedical Imaging and Bioengineering, of the National Institutes of Health, the Peking Union Medical College Scholar project, the Key Project on Inter Governmental International Scientific and Technological Innovation Cooperation in National Key Projects of Research and Development Plan (2016YFE0115400), CAMS Major Collaborative Innovation Project (2016-I2M-1-011), National Natural Science Foundation of China projects (81701742, 81741142) and Beijing Municipal Natural Science Foundation (7161012).

References

1. DeSantis C, Siegel R, Bandi P, Jemal A. Breast cancer statistics, 2011. CA Cancer J Clin. 2011; 61:409–418. [PubMed: 21969133]
2. Siegel R, Naishadham D, Jemal A. Cancer statistics, 2012. CA Cancer J Clin. 2012; 62:10–29. [PubMed: 22237781]
3. Song QK, Li J, Huang R, et al. Age of diagnosis of breast cancer in China: almost 10 years earlier than in the United States and the European Union. Asian Pac J Cancer Prev. 2014; 15:10021–10025. [PubMed: 25520063]
4. Kim Y, Yoo KY, Goodman MT. Differences in incidence, mortality and survival of breast cancer by regions and countries in Asia and contributing factors. Asian Pac J Cancer Prev. 2015; 16:2857–2870. [PubMed: 25854374]
5. Markwalder R, Reubi JC. Gastrin-releasing peptide receptors in the human prostate: relation to neoplastic transformation. Cancer Res. 1999; 59:1152–1159. [PubMed: 10070977]
6. Gugger M, Reubi JC. GRP receptors in non-neoplastic and neoplastic human breast. Am J Pathol. 1999; 155:2067–2076. [PubMed: 10595936]
7. Sun B, Halmos G, Schally AV, et al. Presence of receptors for bombesin/gastrin-releasing peptide and mRNA for three receptor subtypes in human prostate cancers. Prostate. 2000; 42:295–303. [PubMed: 10679759]
8. Halmos G, Wittliff JL, Schally AV. Characterization of bombesin/gastrin-releasing peptide receptors in human breast cancer and their relationship to steroid receptor expression. Cancer Res. 1995; 55:280–287. [PubMed: 7812958]
9. Dalm SU, Sieuwerts AM, Look MP, et al. Clinical relevance of targeting the gastrin-releasing peptide receptor, somatostatin receptor 2, or chemokine C-X-C motif receptor 4 in breast cancer for imaging and therapy. J Nucl Med. 2015; 56:1487–1493. [PubMed: 26251419]
10. Cescato R, Maina T, Nock B, et al. Bombesin receptor antagonists may be preferable to agonists for tumor targeting. J Nucl Med. 2008; 49:318–326. [PubMed: 18199616]
11. Mansi R, Wang X, Forrer F, et al. Evaluation of a 1,4,7,10-tetraazacyclododecane-1,4,7,10-tetraacetic acid-conjugated bombesin-based radioantagonist for the labeling with single-photon emission computed tomography, positron emission tomography, and therapeutic radionuclides. Clin Cancer Res. 2009; 15:5240–5249. [PubMed: 19671861]
12. Ginj M, Zhang H, Waser B, et al. Radiolabeled somatostatin receptor antagonists are preferable to agonists for in vivo peptide receptor targeting of tumors. Proc Natl Acad Sci USA. 2006; 103:16436–16441. [PubMed: 17056720]
13. Varasteh Z, Velikyan I, Lindeberg G, et al. Synthesis and characterization of a high-affinity NOTA-conjugated bombesin antagonist for GRPR-targeted tumor imaging. Bioconjug Chem. 2013; 24:1144–1153. [PubMed: 23763444]
14. Zhang J, Niu G, Fan X, et al. Positron emission tomography using a GRPR antagonist ^{68}Ga-RM26 in healthy volunteers and prostate cancer patients. J Nucl Med. Nov 9.2017 Epub ahead of print.
15. Wolff AC, Hammond ME, Hicks DG, et al. Recommendations for human epidermal growth factor receptor 2 testing in breast cancer: American society of clinical oncology/College of american pathologists clinical practice guideline update. J Clin Oncol. 2013; 31:3997–4013. [PubMed: 24101045]
16. Recommandation for uniform definition of an immunoreactive score (IRS) for the immunohistochemical estrogen receptor detection (ER-ICA) in breast cancer tissue. Pathologe. 1987; 8:138–140. [PubMed: 3303008]

17. Spanu A, Schillaci O, Meloni GB, et al. The usefulness of ^{99m}Tc-tetrofosmin SPET scintimammography in the detection of small size primary breast carcinomas. Int J Oncol. 2002; 21:831–840. [PubMed: 12239623]

18. Liu L, Song Y, Gao S, et al. ^{99m}Tc-3PRGD2 scintimammography in palpable and nonpalpable breast lesions. Mol Imaging. 2014; 13:1–7.

19. Maina T, Bergsma H, Kulkarni HR, et al. Preclinical and first clinical experience with the gastrin-releasing peptide receptor antagonist [^{68}Ga]SB3 and PET/CT. Eur J Nucl Med Mol Imaging. 2016; 43:964–973. [PubMed: 26631238]

20. Stoykow C, Erbes T, Maecke H, et al. Gastrin-releasing peptide receptor imaging in breast cancer using the receptor antagonist ^{68}Ga-RM2 and PET. Theranostics. 2016; 6:1641–1650. [PubMed: 27446498]

21. Halmos G, Wittliff JL, Schally AV. Characterization of bombesin/gastrin-releasing peptide receptors in human breast cancer and their relationship to steroid receptor expression. Cancer Res. 1995; 55:280–287. [PubMed: 7812958]

22. Clément M, Gaétan M, Véronique B, et al. Expression of Gastrin-releasing peptide receptor (GRPR) in breast cancer and its association with pathological, biological and clinical parameters: a study of 1432 primary tumors. J Nucl Med. 2017; 58(9):1401–1407. [PubMed: 28280221]

23. Lin CY, Ding HJ, Liu CS, et al. Correlation between the intensity of breast FDG uptake and menstrual cycle. Acad Radiol. 2007; 14:940–944. [PubMed: 17659239]

24. Sowers MR, Jannausch ML, McConnell DS, et al. Menstrual cycle markers of ovarian aging and sex steroid hormone genotypes. Am J Med. 2006; 119(Suppl 1):S31–S43.

25. La Marca A, Stabile G, Artenisio AC, et al. Serum anti-Mullerian hormone throughout the human menstrual cycle. Hum Reprod. 2006; 21:3103. [PubMed: 16923748]

26. Fleischmann A, Waser B, Gebbers JO, et al. Gastrin-releasing peptide receptors in normal and neoplastic human uterus: involvement of multiple tissue compartments. J Clin Endocrinol Metab. 2005; 90:4722–4729. [PubMed: 15941862]

27. Liu Y. Role of FDG PET-CT in evaluation of locoregional nodal disease for initial staging of breast cancer. World J Clin Oncol. 2014; 5:982–989. [PubMed: 25493234]

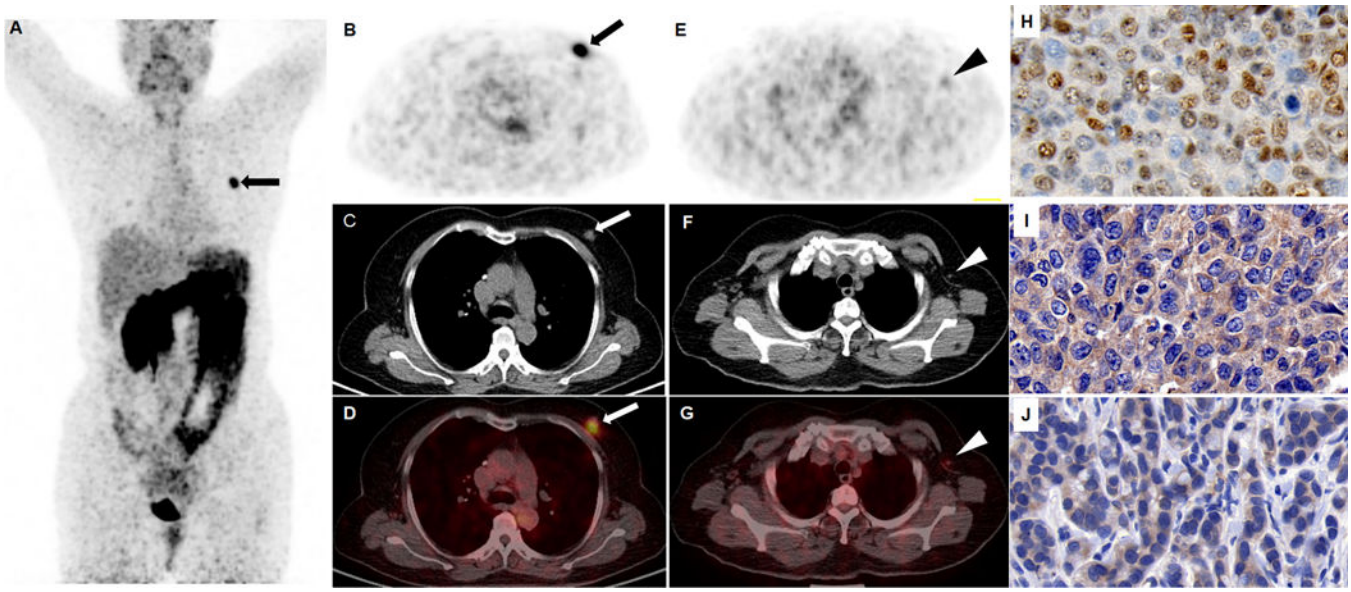

FIGURE 1.

An ER-positive breast invasive ductal carcinoma was clearly visualized (arrow) in the left breast of a 60-year-old post-menopausal patient (A, maximum intensity projection view; B-D, transaxial view of ^{68}Ga-NOTA-RM26 PET, CT and fusion image. The SUV_{max} of the tumor was 9.01 and the SUV_{max} of normal breast tissue was only 0.55). Note that the metastatic lymph node in diameter of 6 mm could also be visualized (arrow head) with elevated ^{68}Ga-NOTA-RM26 uptake with SUV_{max} of 1.2 (E-G). The tumor was stained positively for ER (H) and GRPR (I). The lymph node was also stained positively for GRPR (J).

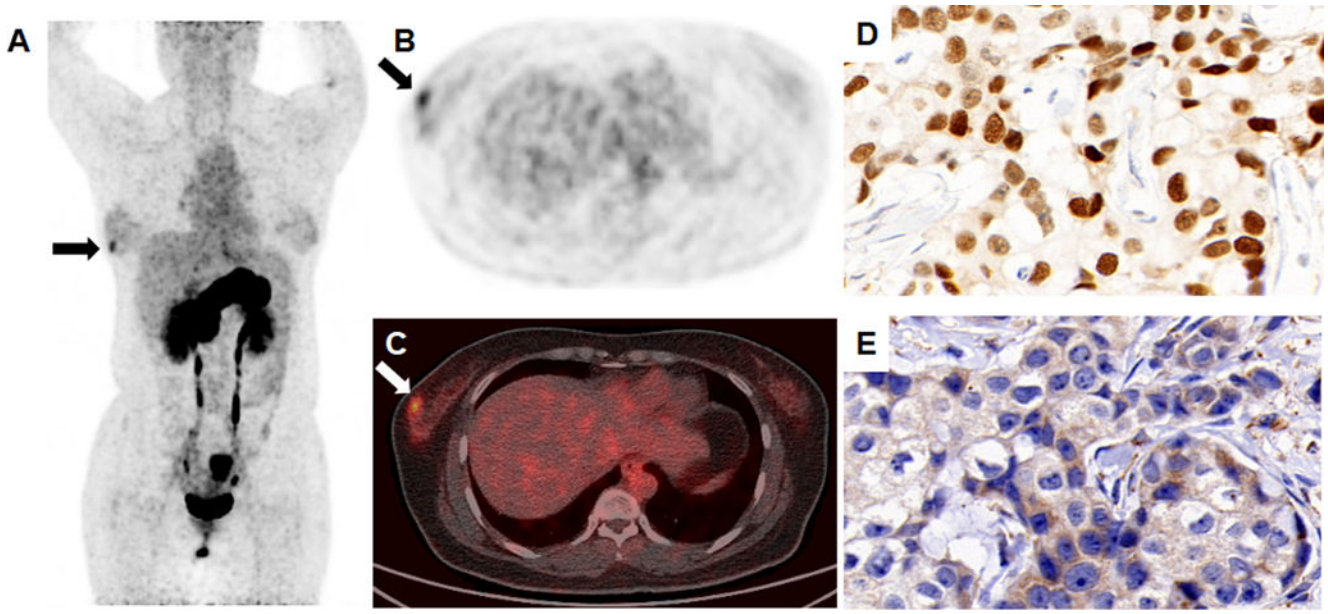

FIGURE 2.

An ER-positive breast invasive ductal carcinoma was detected (arrow) in the right breast of a 30-year-old patient during non-secretory phase of menstrual cycle (A, maximum intensity projection view; B-C, transaxial view of 68Ga-NOTA-RM26 PET and fusion image. The SUVmax of the tumor was 4.02 and the SUVmax of normal breast tissue was 1.72). The tumor was stained positively for ER (D) and GRPR (E).

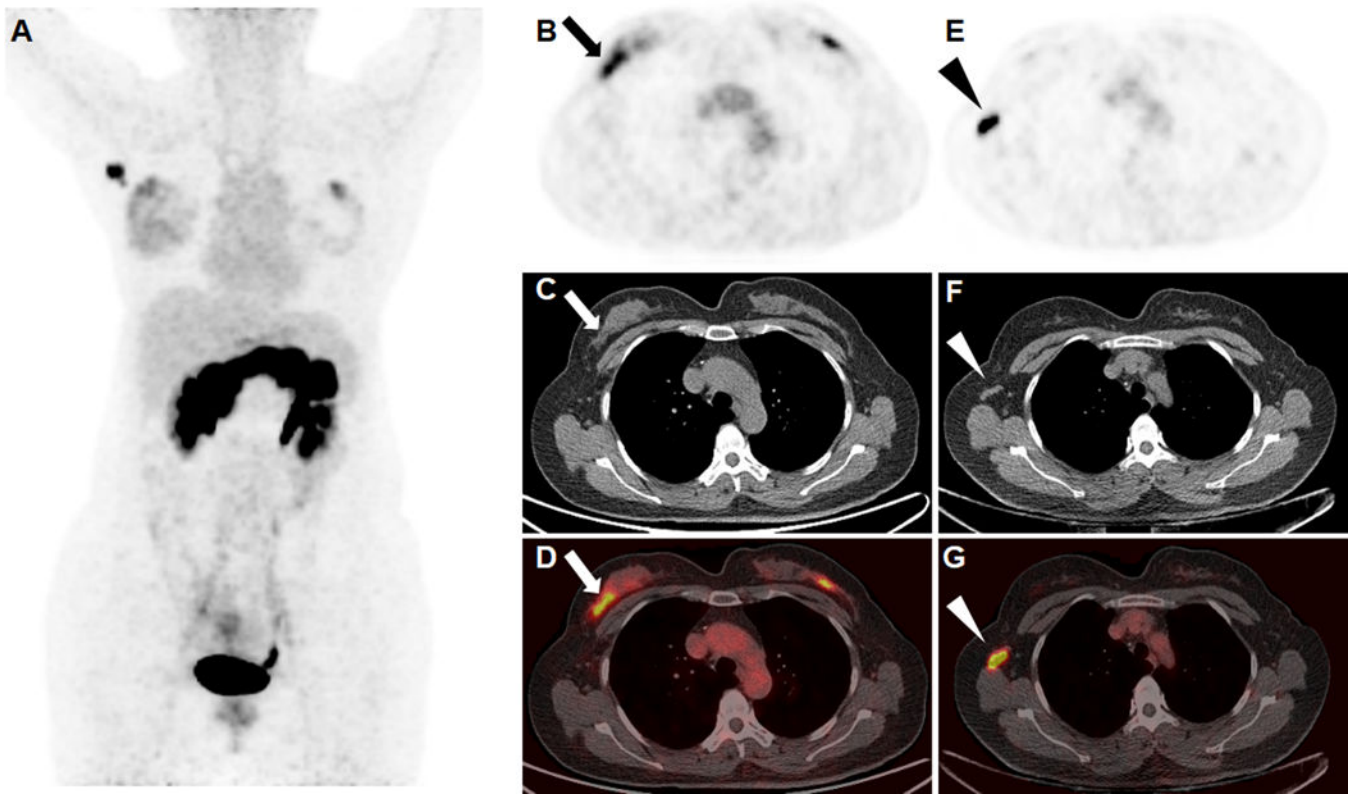

FIGURE 3.

An ER-positive breast invasive ductal carcinoma (arrow) with metastatic lymph node (arrow head) was clearly visualized in the right breast of a 47-year-old patient during the secretory phase of her menstrual cycle (A, maximum intensity projection; B and E, ^{68}Ga-RM26 PET; C and F, CT; D and G, fusion images). The SUV_{max} of the right breast tumor, metastatic lymph nodes, and normal breast tissue were 4.47, 16.14, and 2.20, respectively. An occult lesion was also found on the left breast, but the patient rejected further surgery and the lesion is still under follow up.

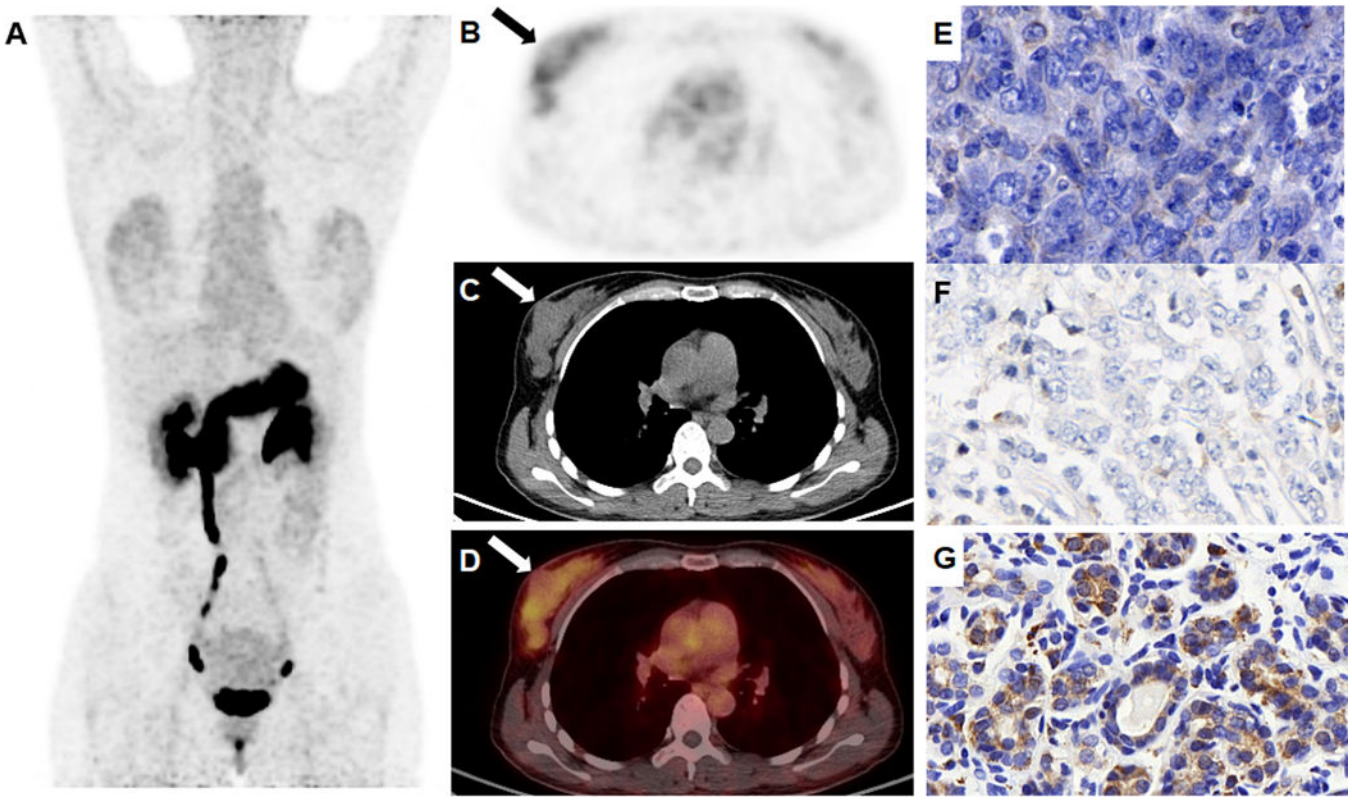

FIGURE 4.

A triple negative breast intraductal carcinoma (arrow) showed uptake lower than the peripheral breast tissue in the right breast of a 34-year-old patient during the secretory phase of her menstrual cycle (A, maximum intensity projection view; B-D, transaxial view of ^{68}Ga-NOTA-RM26 PET, CT and fusion image. The SUV_{max} of the tumor was 2.66 and the SUV_{max} of normal breast tissue was 2.98). The tumor was stained negatively for GRPR (E) and ER (F), and normal breast tissue was stained positively for GRPR (G).

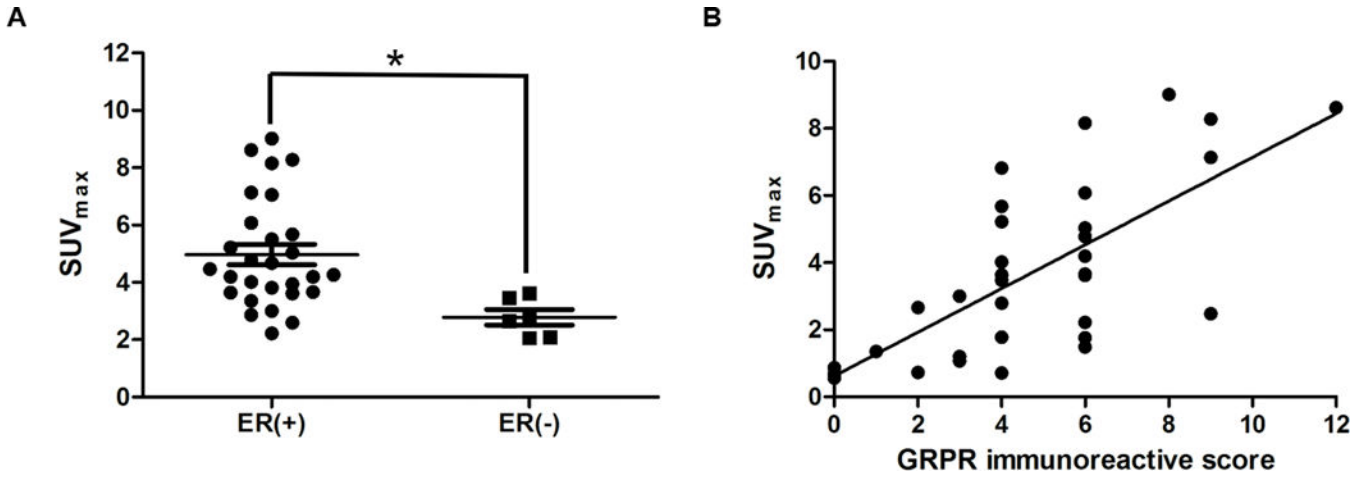

FIGURE 5.

(A) The relationship between the SUVmax of breast cancer and ER status. The SUVmax of ER-positive tumors was 4.97 ± 1.89 compared to 2.78 ± 0.65 in ER-negative tumors ($P < 0.001$). (B) The correlation between 68Ga-NOTA-RM26 PET SUVmax with GRPR expression level of breast cancer and lymph nodes expressed as immunoreactive score ($r = 0.805$, $P < 0.001$).

Clin Nucl Med. Author manuscript; available in PMC 2019 September 01.

TABLE 1

Basic characteristics of the enrolled patients

Patient number	Age	Pathologic diagnosis	Menstrual Phase	LN metastasis	ER stain	Visual diagnosis		Tumor		Breast tissue		T/B ratio	LN	
						Tumor	LN	SUV_{max}	SUV_{mean}	SUV_{max}	SUV_{mean}		Number	SUV_{max}
1	44	invasive ductal cancer	secretory	+	+	P	P	7.14	4.10	3.00	1.80	2.28	1	1.76
2	47	invasive lobular cancer	secretory	+	+	P	P	6.08	4.10	2.18	1.54	2.66	3	6.82
3	47	intraductal carcinoma	secretory	+	−	N	N	2.80	1.72	2.12	1.42	1.21	0	1.35
4	44	intraductal carcinoma	secretory	−	+	N	N	3.64	2.82	2.72	2.04	1.38	0	0.56
5	47	lobular carcinoma *in situ*	secretory	−	+	P	N	8.16	4.64	1.91	1.12	4.14	0	0.87
6	34	invasive ductal cancer	secretory	+	−	N	N	2.66	1.96	2.98	2.54	0.77	0	0.73
7	50	invasive ductal cancer	secretory	+	+	N	N	3.00	1.88	3.22	2.66	0.71	0	1.07
8	47	invasive ductal cancer	secretory	+	+	P	P	5.68	3.74	3.05	2.02	1.85	12	1.78
9	34	fibrous tumor	secretory	−	NA	N	N	3.48	2.04	2.60	1.96	1.04	0	0.57
10	39	invasive ductal cancer	secretory	+	+	P	P	3.94	2.36	2.14	1.46	1.62	4	2.76
11	43	mucinous carcinoma	secretory	+	+	P	P	3.62	2.28	1.08	0.66	3.45	1	1.22
12	52	invasive ductal cancer	secretory	−	+	P	N	2.60	1.48	1.33	0.81	1.83	0	0.81
		fibrous tumor	secretory	−	NA	N	N	1.94	1.08	1.18	0.69	1.57	0	0.54
13	47	invasive ductal cancer	secretory	+	+	P	P	4.47	2.76	2.20	1.22	2.26	1	16.14
14	39	invasive ductal cancer	non-secretory	−	+	P	N	5.22	3.16	1.75	1.00	3.16	0	0.62
15	40	invasive ductal cancer	non-secretory	−	+	P	N	4.02	2.54	1.72	1.04	2.44	0	0.62
16	46	invasive ductal cancer	non-secretory	−	+	P	N	2.22	1.34	1.00	0.70	1.91	0	0.63
17	30	invasive ductal cancer	non-secretory	−	+	P	N	8.62	5.67	2.45	1.76	3.22	0	0.63
18	43	intraductal carcinoma	non-secretory	−	+	P	N	5.04	2.80	1.01	0.75	3.73	0	0.6
19	38	invasive ductal cancer	non-secretory	+	+	P	P	3.66	2.74	2.10	1.50	1.83	1	2.48
20	31	intraductal carcinoma	non-secretory	+	+	P	P	5.50	3.46	1.96	1.48	2.34	3	1.03
21	44	invasive ductal cancer	non-secretory	−	+	P	N	4.19	2.63	1.56	0.98	2.68	0	0.57
22	49	invasive ductal cancer	non-secretory	+	−	P	P	2.07	1.14	1.21	0.64	1.78	2	2.22
23	39	invasive ductal cancer	non-secretory	+	+	P	P	7.05	3.95	1.15	0.79	5.00	1	0.96
24	58	invasive ductal cancer	post-menopausal	−	+	P	N	8.28	5.52	2.01	1.20	4.60	0	0.57

Patient number	Age	Pathologic diagnosis	Menstrual Phase	LN metastasis	ER stain	Visual diagnosis		Tumor		Breast tissue		T/B ratio	LN	
						Tumor	LN	SUV_{max}	SUV_{mean}	SUV_{max}	SUV_{mean}		Number	SUV_{max}
25	58	invasive ductal cancer	post-menopausal	−	+	P	N	4.78	2.64	1.28	0.81	3.26	0	0.68
26	70	invasive ductal cancer	post-menopausal	+	+	P	P	4.20	2.32	1.31	0.73	3.18	1	0.71
27	60	invasive ductal cancer	post-menopausal	+	+	P	P	9.01	5.98	0.55	0.35	17.09	1	1.2
28	47	invasive ductal cancer	post-menopausal	−	+	P	N	3.36	1.68	2.04	0.94	1.79	0	0.65
29	64	invasive ductal cancer	post-menopausal	−	+	P	N	4.68	2.98	1.74	0.98	3.04	0	0.7
30	63	invasive ductal cancer	post-menopausal	+	−	N	P	2.10	1.26	1.42	0.93	1.35	1	1.23
31	65	invasive ductal cancer	post-menopausal	+	−	P	P	3.62	2.16	2.00	1.24	1.74	13	1.49
32	40	invasive ductal cancer	post-menopausal	−	+	P	N	4.27	2.53	1.01	0.53	4.77	0	0.49
33	63	invasive ductal cancer	post-menopausal	−	−	P	N	3.45	1.88	1.23	0.79	2.38	0	0.65
34	68	invasive ductal cancer	post-menopausal	+	+	P	P	2.87	1.66	1.22	0.79	2.10	1	2.01
35	71	invasive ductal cancer	post-menopausal	−	+	P	N	3.82	2.15	1.39	0.75	2.87	0	0.90

LN: lymph node; ER: estrogen receptor; T/B : tumor to background; SUV_{max}: maximum standardized uptake value; SUV_{mean}: mean standardized uptake value; P: PET-positive; N: PET-negative; NA: non-available